Structural Behavior of GFRP Reinforced Recycled Aggregate Concrete Columns with Polyvinyl Alcohol and Polypropylene Fibers

By

UMER RAFIQUE

(NUST 2018-277043)

This thesis is submitted in partial fulfillment of
the requirements for the degree of

Master of Science

in

Structural Engineering

National Institute of Civil Engineering (NICE)

School of Civil and Environmental Engineering (SCEE)

National University of Sciences & Technology (NUST)

Islamabad, Pakistan

October 2021

This is to certify that Thesis entitled

Structural Behavior of GFRP Reinforced Recycled Aggregate Concrete Columns with Polyvinyl Alcohol and Polypropylene Fibers.

Submitted by

Umer Rafique

Has been accepted towards the partial fulfillment

of

the requirements

for award of degree

of

Master of Science in Structural Engineering

Thesis Supervisor

_____

(Prof. Dr. Ather Ali, PhD) Assistant Professor of Structural Engineering NUST Institute of Civil Engineering (NICE)

School of Civil and Environmental Engineering (SCEE)
National University of Sciences and Technology (NUST)

August 2020, Islamabad Pakistan

THESIS ACCEPTANCE CERTIFICATE

Certified that final copy of MS/MPhil thesis written by Mr. Umer Rafique, Registration No. 00000277043, of MS Structural Engineering 2018 Batch (NICE) has been vetted by undersigned, found completed in all respects as per NUST Statutes/Regulations, is free of plagiarism, errors, and mistakes and is accepted as partial fulfilment for award of MS/MPhil degree. It is further certified that necessary amendments as pointed out by GEC members of the scholar have been incorporated in the said thesis.

Signature_____

Name of Supervisor Dr. Ather Ali

Date: _____

Signature (HoD)_____

Date: _____

Signature
(Dean/Principal)_____

Date:_____

ACKNOWLEDGEMENT

"**In the name of Allah, the most beneficent the most merciful**"

Foremost, I would like to express my earnest thankfulness to my supervisor Dr. Ather Ali for his persistence, interest and massive knowledge. His guidance helped me in all the time of research and writing this thesis. His pleasing and welcoming behavior facilitated me to discuss my point of view on the topic in detail and resolved my queries to my full satisfaction.

Here, it is worth mentioning that the completion of this study was possible due to the assistance of many dedicated and helpful colleagues. In addition to my supervisor and committee members, I am also thankful to my friends specially Engr. Ali Raza for supporting me all the way through my study.

Finally, I extend my profound gratitude to my family members, for all that they meant to me throughout this critical time of completion of my study.

ABSTRACT

This research had the purpose of demonstrating the axial compressive behavior shown by GRFC columns by making a total of five circular columns (with height and cross section of 1150mm and 250mm respectively) and having them tested under the axial concentric loading. The micro fibers incorporated into concrete were of two separate kinds namely polypropylene fibers (PPF) as well as polyvinyl alcohol fibers (PVA). The transverse confinement provided was of two different types (GFRP hoops as well as the GFRP spirals). In order to explore the GFRP hoops' efficiency, the spacing was kept at 75 mm, 150 mm, and 250 mm, respectively. Whereas, spacing of 75mm as well as 38mm was used to examine the GFRC spirals' efficiency. The axial strength as well as ductility indices were higher for the GRFC columns that were confined with the GFRP spirals. Moreover, a detailed extensive finite element modeling (FEM) was carried out by taking into account the influence shown by hybrid fibers utilizing a revised and improved concrete damaged plastic (CDP) model. The suggested FEM showed high accuracy in capturing axial response as well as the cracking behavior shown by GRFC columns. This study resulted in putting forward a new and unique empirical model in order to capture axial strength shown by the GRFC columns taking into account the effect shown by GFRP bars as well as lateral confinement of the GFRP hoops/spirals.

TABLE OF CONTENTS

LIST OF FIGURES

LIST OF TABLES

Chapter 1

INTRODUCTION

1.1 General

Following the polymerization of fibers, the composite reinforcing materials produced industrially are generally known as Fiber Reinforced Polymers (FRPs). An alternative name for these products is Fiber Reinforced Plastics (FRPs). There is an extensive utilization of fiber reinforced polymers, its different types being employed in comparison to traditional steel reinforcement in the reinforced concrete structures owing to few superior characteristics. As we know that heavily reinforced concrete structures are subjected to different loading conditions and environmental constraints, therefore it is essentially required to learn response of structure under different loading condition. Owing to anticorrosive nature, lightweight, non-magnetic and electrical resistivity in addition to high tensile strength and lower thermal conductivity, glass fiber reinforced polymers (GFRP) are generally preferred as reinforcing bars in structural elements. As an alternative to steel bars in structures, GFRP bars are being prove to be a feasible substitute. Owing to its non-magnetic behavior and its non-conductivity, some of the best utilization of GFRP materials is near sensitive instruments in laboratories and hospitals. With swelling world population, massive urban development, additionally the economic condition faced by the developing states, induced greater attention towards employment of the recycled coarse aggregate (RCA) acquired from the building and demolition wastes. To further delay cracking of concrete core and increase axial strength, polyvinyl alcohol and polypropylene fibers are added to concrete mix.

In this research, all the three basic approaches i.e. experimental, numerical and analytical are used to study the response of structure. Experimental testing is the best approach to know the actual structural behavior especially in small structures. Experimental investigation of heavy and complex structures is pricey, cumbersome and strenuous. It is very hard to create factual loading conditions and the setup that matches the real scenario to which the structure is subjected. Alternative approaches, to predict the response of civil structures are the Numerical and Analytical ones. Numerical approaches are simple and convenient to follow and flexile for any alteration to design and subjected conditions etc. Linear and Nonlinear Finite Element Analysis (FEA) is the most extensively used numerical approach for analysis of civil engineering structures. Commonly used software's for such type of analysis are ABAQUS, ANSYS, STRAND7 and SEISMOSTRUCT. The use of FEA Software for numerical analysis of structures is immensely increasing due to shift towards technology, advancement in data processing servers and the growing trend towards use of software for structural analysis and design. The effective use of FEA Package and investigating limitations of each computer software is essential for an efficient design and analysis. The analytical approach comprises of producing empirical relation, by processing results obtained from experimental testing and numerical modelling. It gives the simplest solution in the form of empirical relation to generate results without even casting or modelling.

This research comprises of studying structural response of axially loaded concrete columns comprising recycled aggregate, polyvinyl alcohol and polypropylene fibers and reinforced with GFRP bars. In this study loading applied on specimens is concentric in all cases. For testing purpose five cylindrical column specimens were casted with varying pitch of transverse reinforcement to study their failure and compare their results with those of assembled models in ABAQUS software. Longitudinal reinforcement is

same in all samples, while transverse reinforcement in three of them is spiral and the remaining two have hoops. The assembled models in ABAQUS predicted same collapse behavior as visible in tested specimens.

1.2 Research Problem

Nowadays, concept of recycling or green concrete is in full swing. With ever increasing pace of urbanization there is a need to reutilize demolished structure's waste, to minimize landfill and environmental pollution. GFRP bars as longitudinal and transverse reinforcement along with ordinary concrete is commonly used in corrosive environment to enhance structural life and better ductile behavior in seismic condition. But till now, literature is deficient regarding combined use of GFRP bars, RCA and fibers in columns subjected to concentric loading. Sole purpose is to study the overall effect of all these building blocks on overall strength and performance under loading.

1.3 Relevance to the national needs

GFRP bars are replacing ordinary steel reinforcement in heavy structures to minimize overall structural weight, with almost same axial compressive strength at low concrete cover. Although, it is used in retaining walls along seashore and columns of harbor platform at some places here in Pakistan but still structural designers are reluctant to incorporate these materials because of limited or very little research on locally available material. GRFC columns shows a bit lower compressive strength for same volumetric ratio of GFRP bars as of steel reinforcement, but overall ductility is enhanced which is main focus in structures subject to seismic loading. By incorporating hybrid fibers brittle failure of concrete is extensively minimized. These types of columns are cost effective, environment friendly and able to perform better than steel reinforced columns under varying eccentric loading.

1.4 Research Methodology

Research methodology comprises of below mentioned steps.

a. Recycled aggregate collection by crushing cylinder having 30-40 MPa compressive strength.
b. Two types of fibers (PVA and PPF) are arranged to add in concrete mix.
c. Concrete mixture used to prepare specimens had average compressive strength of 28.7 MPa with standard deviation of 2.14 MPa at 28 days testing.
d. Five specimens of dia. 250 mm and height 1150 mm were casted of this concrete mix.
e. E-glass fibers were used for the preparation of GFRP bars. Transverse reinforcement in three of the specimens was hoop ties at 75 mm, 150 mm and 250 mm pitch while in other two specimens was spiral at pitch of 38 mm and 75 mm.
f. Load was applied at the rate of 0.003 mm/s to generate complete curve even after cracking.
g. FEM software ABAQUS was used to assemble these specimens, in which concrete damage plastic model (CDP) was assigned to concrete. Properties of HFRC was precisely defined.
h. Crack pattern given by FEA was compared with experimental results to validate FEA results.
i. Finally, empirical relation given for ordinary concrete embedded with GFRP bars was modified to incorporate effect of confinement provided by transverse reinforcement recycled aggregate and hybrid fibers.

1.5 Research Objectives

Primary objective of this exercise is to study the compressive strength and ductility of columns embedded with GFRP bars as compared to ordinary concrete. The factors studied in specimens under concentric loading are

a. The effect of incorporating recycled coarse aggregate on compressive strength.
b. The effect of replacing steel reinforcement with GFRP bars on compressive strength along with complete behavior under nonlinear loading.
c. Changes in compressive strength and crushing pattern on varying pitch of transverse reinforcement in both cases of spirals and hoops.
d. Minimizing variation in empirical relation outcome to experimental results so that prescribed relation could be further employed to find compressive strength of concrete columns.

Chapter 2

LITERATURE REVIEW

2.1 Introduction

Loading capacity and ductility of ordinary steel reinforced concrete structural elements is reduced owing to steel corrosion, resulting in narrowed performance chart and escalated maintenance expenditures. Substituting the steel reinforcing bars with glass fiber reinforced polymer (GFRP) bars has been observed to be not only a suitable but also a practically employable solution to this problem, because of its higher tensile strength and impervious nature to corrosive environment in addition to lower density to mass ratio (Raza et al. 2020a). The lifespan of the structures incorporating GFRP bars is amplified in an aggressive environment at the cost of low maintenance expenses during its lifecycle (Benmokrane et al. 2006, Jiang et al. 2018, Raza 2019).

These are the chief reasons of its acceptance in construction industry, helping to patch trust deficit of regulating authorities. Brittleness of concrete increases with increase in its compressive strength leading to low ductility and catastrophic failure. This is a serious drawback of concrete to be used in structures. These short comes of strength and ductility of concrete can be counterbalanced by adding short hybrid fibers (Bayramov et al. 2004, Paultre et al. 2010, Raza 2020). Thus, to enhance the characteristics of concrete to boost the seismic response of various structural elements like columns different types of fibers would be added in plain concrete (Pang et al. 2019). For this purpose, instead of steel fiber plastic fibers of two types knowingly, Polyvinyl Alcohol (PVA) and Polypropylene fibers (PPF) are used in this study to curtail the brittle nature of the concrete columns embedded with GFRP bars.

These fibers can transfer the loads through the cracks and boost the toughness and restrict the crack propagation in concrete (Darole et al. 2013). Thus, fibers act as the secondary reinforcement to mitigate cracking in concrete. Although fibers do not remarkably amplify the compressive strength of concrete, they improve the flexural stiffness and tensile capacity of concrete (Zhang et al. 2018)

Apart from for axial compressive capacity, GFRP reinforcement and steel exhibit, almost same response. Whereas, 7% less axial compressive capacity has been observed for glass fiber reinforced recycled aggregate fiber incorporated (GRFC) columns (Afifi et al. 2014). However, an increase in column's ductility has been observed GFRP bars substitute the steel bars in equal amount. The underlying reason of this increase, in addition to linear elastic behavior, is the higher strain capacity of the GFRP bars (Hadi et al. 2016). Post-peak portion of curve comparison shows that, superior confinement is provided by GFRP-RC column as compared to the steel reinforced columns, which is due to its extreme lateral confinement (Tobbi et al. 2014).

Using recycled coarse aggregates from building construction and destruction waste can reserve natural aggregate resources, reduce landfill demand, and help in building sustainable environment (Wang et al. 2021) by significantly reducing carbon footprint (Liu et al. 2020). Incorporating recycled coarse aggregate (RCA) in new construction reduces freight charges of aggregate and landfill space for construction solid waste. Mechanical properties show that concrete prepared using RCA have reduced compressive strength and increased porosity and water absorption in contrast to natural aggregate concrete (NAC). While conversely, RCA concrete depicted higher ductility than NAC (Ma et al. 2013). Usage of recycled aggregate concrete (RAC) in construction is supported by a limited number of studies (Raza et al. 2021).

The blend of FRPs and RAC in comparison to that of steel bars and RAC will present enhanced performance level owing to almost similar modulus of elasticity of both FRPs and RAC (Raza and Rafique 2021). Now a days, researchers linked to structural engineering are focusing to utilize FRP bars in reinforced concrete construction. In contrast to steel bars reinforced slender columns, GFRP bars reinforced columns show lower level of lateral deflection (Hales et al. 2017). Due to linear elastic behavior of FRP-RC columns up till collapse, PM interaction curve does not give balance point (Choo et al. 2006). Furthermore, empirical relation to calculate minimum reinforcement ratio in case of FRP-RC columns are put forward in literature (Choo, Harik et al. 2006).

The area below the PM interaction curve is although lower in case of GFRP reinforced columns as compared to ordinary steel reinforced columns but for varied loading conditions ductility of specimens is enhanced (Hadi, Karim et al. 2016). Results collected from tests by (Mohamed et al. 2014) showed that, protruding of main/longitudinal reinforcement was the chief collapse reason at 0.7% of volumetric ratio of lateral ties, whereas for volumetric ratio of 1.5% to 2.7%, breaking of lateral ties and eventually crushing of solid concrete core was the overall reason of collapse. Various empirical models incorporating the effect of longitudinal GFRP reinforcement are part of literature to visualize the axial capacity of GRFC columns under compressive load (Afifi, Mohamed et al. 2014, Mohamed, Afifi et al. 2014, Hadi, Karim et al. 2016).

Structural response of RAC compression members in light of many studies is part of literature(Kim et al. 2013, Abdelrahman and El-Hacha 2014, Li et al. 2015, Li et al. 2017, Li et al. 2018). In a study carried out by (Choi and Yun 2012) the axial strength shown by RC columns casted with RAC showed 6-8% lesser value in contrast to ordinary concrete columns. Moreover, the necessity of free water adsorbed on the surface of recycled coarse aggregate is fulfilled by presoaking of recycled coarse

aggregates. After assessing the response of RAC columns under compressive loading (Hastemoglu 2015) suggested to entirely remove the binder from RCA by different crushing stages. In addition, fine particles attached to RCA should be washed off. A lot of studies on steel tube columns filled with RAC showed that such type of casted specimens showcased decent structural response under diverse sorts of loading. (Wang et al. 2015) illustrated that the compressive strength of RAC filled steel tube columns decreased with increase in replaced amount of RCA in RAC. Enhanced durability and curbed maintenance cost of RAC columns is due to transverse confinement provided by FRPs sheet or bars (Abdelrahman and El-Hacha 2014). It is deduced from study of (Boumarafi et al. 2015, Xu et al. 2017) that, in order to achieve improved mechanical and durability performance of RAC columns combined usage of RAC with FRPs is viable solution.

To investigate the structural response, study the delicate failure mechanism and to apprehend the interaction curve of individual FRPs or in combination with concrete, in least possible time and at minimum cost, finite element modelling is one of the most productive tool (Shi et al. 2012). Finite element analysis and test results showed that instead of strength limits of constituents, the structural strength of GFRP-RC columns is mostly controlled by peak deflections along with local buckling (Lu 2011, Silva et al. 2011). The structural behavior of GFRP reinforced columns samples under buckling load can be effectively simulated by FEM (Boscato and Ientile 2018). Finite element based simulations were performed through ANSYS (Turvey et al. 2006) and ABAQUS (Elchalakani et al. 2018) to predict response of short columns reinforced with GFRP bars and performed calculations regarding specimens' failure and post-buckling behavior develop a close agreement among test results and finite element predictions.

(Hany et al. 2016, Raza 2019, Elchalakani et al. 2021) stated that FEM tool can anticipate load-deflection curve and failure patterns with adequate precision.

2.2 Scope and Significance of Research

Literature is unavailable regarding structural response of GRFC columns under compressive loading. The intention of this study is to observe the structural behavior of GFRP-RC concentrically loaded columns through experimental results and nonlinear finite element-based investigation for upgrading sustainable environment. Study is aligned to determine the result of variation in the vertical pitch of transverse ties, incorporation of recycled coarse aggregate, plastic fibers, and loading scenario to which specimens are subjected. Modified concrete damaged plasticity (CDP) model was utilized to properly define the properties of recycled aggregate and plastic fibers in FEM. To evaluate the compressive bearing capacity of GRFC columns an empirical model was proposed. Findings from this study will be supportive for the building industry to design and analyze the GRFC columns that are economical, utilize construction solid waste materials, eco-friendly and sustainable by employing recycled aggregate.

Chapter 3

RESEARCH METHODOLOGY

3.1 Specifications of Concrete Blend

Portland cement of grade 43R is used to prepare hybrid fiber-reinforced concrete (HFRC). Recycled coarse aggregate to be used in this concrete mix is obtained from the crushing of concrete cylinders casted at least six month or one year ago of compressive strength 30 MPa to 40 MPa. Extreme size of RCA was up to 10 mm. Characteristic properties of recycled coarse aggregate are presented in Table 3-1. Fineness modulus of fine aggregate used in the mixture was 2.3. Plastic fibers of two kinds namely polyvinyl alcohol (PVA) and polypropylene (PPF) were added to blend. The cross-sectional diameter and length of PVA were and 39 µm and 8 ± 1 mm respectively. Likewise, the diameter and length of the other fiber PPF were 24 µm and 12 ± 1 mm, respectively. A superplasticizer, Sika ViscoCrete®-3100 was used to enhance workability and homogeneity of concrete mix. Slump value obtained from slump test according to ASTM C143/C143M-15, of fresh mix came out to be 105 mm. Various characteristics of concrete elements are mentioned in tabular form in Table 3-2.

Table 3-1 Features of Recycled Aggregate

Parameter	Value
Dry density	1340 kg/m^3
10% fine value	131
Water absorption at 24 hours	9.65%
Specific gravity	2.28
Maximum size	10 mm
Minimum size	4.75 mm

Table 3-2 Ingredients of Concrete (kg/m^3)

Cement content	Coarse recycled aggregates	Fine aggregates	Water content	PPF	PVA	Super-plasticizer	Water to cement ratio
474.23	1087.83	595.57	172.92	1.79	2.5	2.28	0.36

Six concrete cylinders of dimension 150 mm X 300 mm were casted to discover unconfined compressive strength of concrete blend. On the same day as of testing columns, concrete cylinders were also tested. Mean axial capacity showed by these casted cylinders came out to be (28.7 ±2.14) MPa, as 2.14 MPa is standard variance.

Bar #3 was used as transverse reinforcement while bar #4was used as longitudinal reinforcement. The GFRP reinforcing bars used in this study were with a coating and ligatures, consist of E-glass fibers soaked in thermosetting vinyl ester resin and other additives. Likewise, 80% amount of fiber was collected from SupAnchor® for fabrication purpose. The mechanical and geometrical characteristics of glass fiber reinforced polymer bars utilized in this study are presented in Table 3-3.

Table 3-3 Properties of GFRP Bars

Bar number	Nominal diameter (mm)	Nominal area (mm^2)	Nominal tensile strength (MPa)	Tensile elastic modulus (GPa)	Ultimate tensile strain (%)
#4	12.7	126.7	845	50	2.15
#3	9.5	70.8	725	45	2.42

3.2 Fabrication of testing specimens

Circular HFRC compression members, five in number were prepared for study purpose. Prepared samples were tested to discover the outcome of pitch variation of transverse

ties, PVA & PPF fibers, recycled aggregate and loading circumstances to which columns are subjected. Volumetric ratio of 0.50%, 0.71% and 1.42% was achieved by providing lateral ties at pitch of 250 mm, 150 mm and 75 mm respectively. According to (Maranan et al. 2016). Pitch of GFRP transverse ties was provided to make sure elastic buckling of GFRP longitudinal bars. The inner measurements of column casing formwork were 250 mm diameter and 1150 mm height. 20 mm of concrete cover furnished in all specimens. Figure 1 shows cross sectional specifics of the control specimen with transverse pitch of 75 mm. Table 3-4 shows the casted specimens and geometric details of the present study.

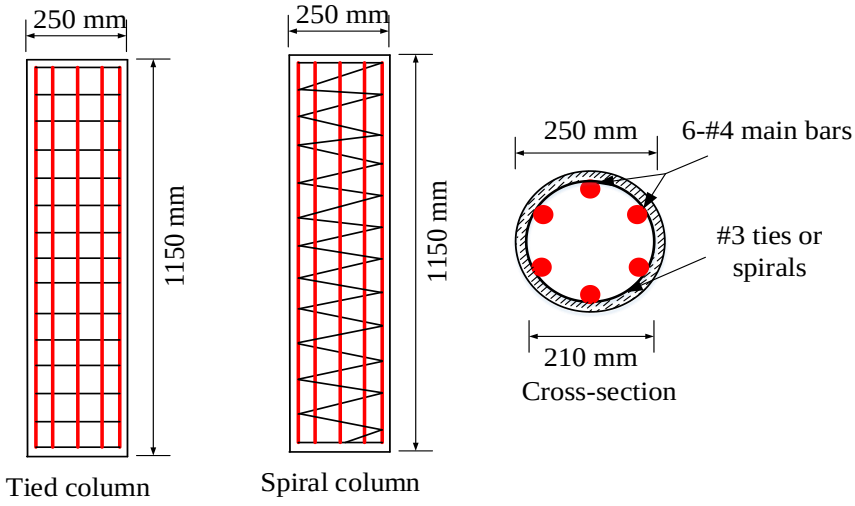

Figure 1 Geometry of Fabricated Specimen

Table 3-4 Test Matrix

Specimen label	Longitudinal reinforcement		Transverse reinforcement	
	Bars and diameter	Reinforcing ratio (%)	Bars, diameter, and spacing	Volumetric ratio (%)
G6-H75	6 bars of 12.7 mm diameter	1.57	9.5 mm ties @ 75 mm c/c	1.42
G6-H150	6 bars of 12.7 mm diameter	1.57	9.5 mm ties @ 150 mm c/c	0.71
G6-H250	6 bars of 12.7 mm diameter	1.57	9.5 mm ties @ 250 mm c/c	0.50
G6-S38	6 bars of 12.7 mm diameter	1.57	9.5 mm spirals @ 38 mm c/c	2.84
G6-S75	6 bars of 12.7 mm diameter	1.57	9.5 mm spirals @ 75 mm c/c	1.42

Formwork comprises of 5 mm thick PVC pipes with inner diameter 250 for molding columns. Concrete was poured after lowering reinforcement cage in the formwork and throughout the pouring task formwork was vibrated nonstop using poker.

3.3 Testing, formwork and Testing Instrument Particulars

Hydraulic press based on loading with a topmost applied load of $5x10^3$ kN was availed for applying load at the pace of 3×10^3 mm/s over columns. To evenly distribute the applied load, both ends were leveled after stuffing pores and lastly steel collars of 100 mm width and 10 mm thickness were positioned over it. Additionally, to avoid early collapse, steel caps are linked to top and bottom, helpful to confine concrete at end points. LVDTs were connected longitudinally to the column about its circumference. Statistics collectors linked to testing apparatus record stats of load, strain, and vertical deflection. Fracture patterns and failure patterns of the tested samples were videotaped. Figure 2 presents the details of testing machine.

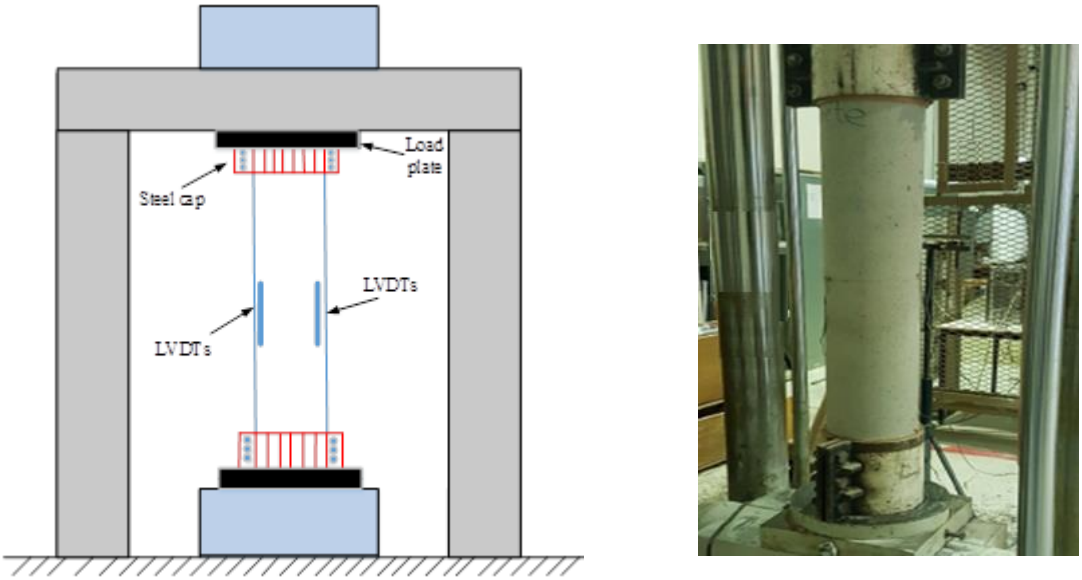

Figure 2 Testing Setup and Arrangement

3.4 Finite element modelling

With the help of the suggested FEM and usage of ABAQUS software, the preliminary stiffness, peak failure mechanism, peak load collapse spreading pattern, and stiffness decline after cracking have been measured. The Calibration of FEM models was based on experimental findings of the control specimen (G6-H75). The 3-D solid section was assigned to model concrete blend while 3-D wire element was used for the modelling of GFRP. To simulate complex collapse behavior of HFRC, the suggested model as input was revised concrete damage plastic (CDP) model. The translatory motion was exclusively restrained at the lower end of the specimen, however rotation in all directions was permitted at this end. On the other hand, both the rotational and translational motions, were permitted at the upper end, in either direction. The "embedded region" restraint served as a marker to mark off the bondage between HFRC and reinforcing material. This embedded region serves as a linker and works to link the degree of freedoms (DOF) of both, the wire/truss elements and the 3D stress section of concrete (Raza 2019). A uniformly distributed load (UDL) was placed on the upper surface of the column under displacement control technique. This endorsed/ratified the

actual load condition as applied during testing. By the use of “tie constraint”, the specimen was attached at both ends with steel plates which were 50 mm in thickness. This was done in order to apply the boundary conditions. Figure 3 depicts the modelled sample along with the end conditions.

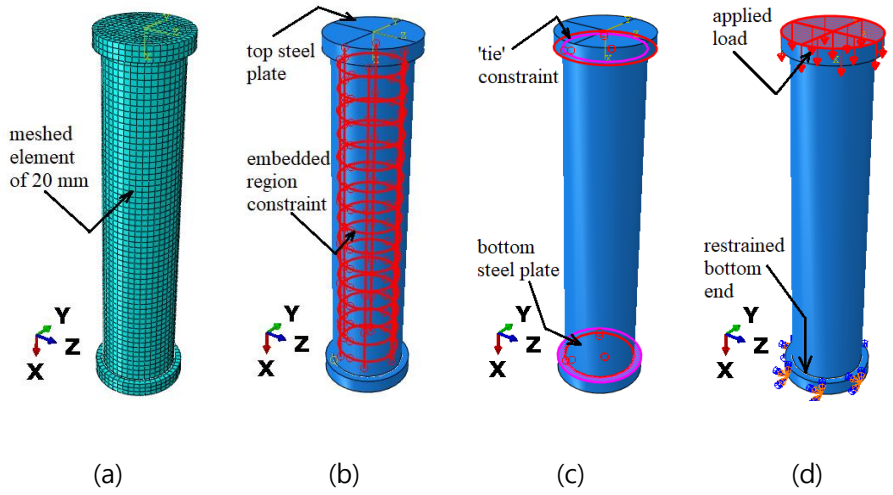

Figure 3 Specimen Modeling in ABAQUS (a) Meshing (b) Inter connection of HFRC & GFRP (c) Load Plates Linked to Column (d) End Conditions for Assembly

3.5 HFRC Modeling

Most important step in predicting structural response of concrete elements is proper defining of HFRC properties in modelling software. Elastic modulus taken from $4734\sqrt{f_c'}$ (ACI-318 1995) and poison’s ratio of constant 0.2 (Chi et al. 2014) were ascribed for linear elastic response of HFRC. f_c' ‘the compressive strength of HFRC is assigned a value of 28.7 MPa as obtained from testing control specimen. Concrete damage plasticity model with endorsed amendments as prescribed by (Chi et al. 2017) was utilized to simulate complicated collapse behavior of HFRC. Although the model developed by (Chi, Xu et al. 2014, Chi, Yu et al. 2017) had its utility when hybrid fiber (steel-polypropylene) reinforced concrete are employed, nevertheless, this model was utilized in the current study by bearing in mind that, with slight variations in the mechanical characteristics among FRC, the strengthening behavior of steel fibers and

stiff PVA fibers in the concrete, is similar. Following extensive assessment and comparative study of experimental results and predicted response, implementation of Chi model (Chi, Xu et al. 2014, Chi, Yu et al. 2017) for numerical modeling of HFRC with PVA-PP fibers is considered realistic with suitable exactness.

3.5.1 Plasticity Behavior of HFRC

Five variables namely, eccentricity (e), viscosity (μ), yielding surface shape factor (K_c^{hf}), HFRC dilation angle (ψ) and ratio of peak biaxial to uniaxial compressive stress ($\sigma_{bo}^{hf}/\sigma_{co}^{hf}$) are required in defining CDP model to simulate plastic response of HFRC.

For both plain and HFRC, the assigned value of eccentricity is always 0.1 (Chi, Yu et al. 2017). The factor $\sigma_{bo}^{hf}/\sigma_{co}^{hf}$ in the CDP model, is designated as the peak biaxial to uniaxial compressive stress ratio, and can be given by Eq. (1) (Chi, Yu et al. 2017) assigned 1.48 as its value in numeric.

$$\frac{\sigma_{bo}^{hf}}{\sigma_{co}^{hf}} = \frac{k_t^2}{0.132k_c}\left[\left(0.728 - \frac{0.749}{k_t}\right) + \sqrt{(0.728 - \frac{0.749}{k_t})^2 + \frac{0.03}{k_t^2}}\right] \quad (1)$$

The mark-up factors for compressive peak and tensile strength in equation 1 are k_c and k_t, respectively, where the coefficient k_c, for HFRC, has not yet been defined/characterized, due to the research gap/lag. Thus, (Chi, Xu et al. 2014) has defined the relation of these coefficients as mentioned in equation 2 and 3.

$$k_c = 1 + 0.056\lambda_{PVA} \quad (2)$$

$$k_t = 1 + 0.080\lambda_{PVA} + 0.132\lambda_{PPF} \quad (3)$$

The indices for fiber reinforcement for PVA and PPF in the equation 3 are the variables λ_{PVA} and λ_{PPF}, respectively, each of which is calculated as mentioned in equations 4 and 5 respectively.

$$\lambda_{PVA} = V_{PVA}\left({}^{l_{PVA}}/_{d_{PVA}}\right) \quad (4)$$

$$\lambda_{PPF} = V_{PPF}\left({}^{l_{PPF}}/_{d_{PPF}}\right) \quad (5)$$

Where,

V_{PVA} = Volumetric component of PVA

V_{PPF} = Volumetric component of PPF

l_{PVA} = Mean length of polyvinyl alcohol

l_{PPF} = Mean length of polyethylene fibers

The range of shape factor(K_c) varies in between 6.4 x 10^{-1} to 8.0 x 10^{-1} for plain concrete (Lu 2011, Hadhood et al. 2017). Plain concrete demonstrates a strong relation, at lower stresses, with the test outcomes of compressive strength. Further ahead, for increased compressive stresses, the concrete displays added suitable relation when the value of shape factor is 0.7 (Chi, Yu et al. 2017). Thus, the equation for K_c^{hf} is possible to be expressed in respect of boosting coefficient for both compressive plus tensile meridian (Chi, Xu et al. 2014, Chi, Yu et al. 2017).

$$K_c^{hf} = K_c\left(\frac{k_t}{k_c}\right) \quad (6)$$

The stress flow rule is almost controlled by dilation angle ψ taken as a significant constraint. With a reduction in dilation angle ψ , it was observed that, in HFRC, a slight volumetric plastic strain developed, causing better confinement of the concrete matrix. The relation of variable λ_{PVA} and λ_{PPF} is stated in equation 7 for dilation angle of HFRC (ψ^{hf}) (Chi, Yu et al. 2017).

$$\psi^{hf} = \psi(1 - 0.861\lambda_{PVA} - 0.097\lambda_{PPF}) \quad (7)$$

3.5.2 Behavior of HFRC Under Compression

The total strain induced in concrete is separated into pre-peak (elastic) strain and post peak (plastic) strain for the characterization of irreversible and nonlinear cracking of concrete, under the elastoplastic philosophy.

$$\varepsilon = \varepsilon^{el} + \varepsilon^{pl} \tag{8}$$

In the CDP model there are two variables to imitate the collapse of concrete, known as the uniaxial tensional damage factor (d_t) and uniaxial compressional damage factor (d_c). From Figure 4, the plain concrete is subjected to the compressive stress and this compressive stress can be expressed by Eq. (9).

$$\sigma_c = (1 - d_c)E_o\left(\varepsilon_c - \varepsilon_c^{pl}\right) \tag{9}$$

Here the elastic modulus of concrete, E_o is calculated according to (ACI-318 1995). ε_c is the concrete strain under compression and ε_c^{pl} is the concrete strain within plastic zone. The factor d_c can be found by Eq. (10) stated by (Y 2006).

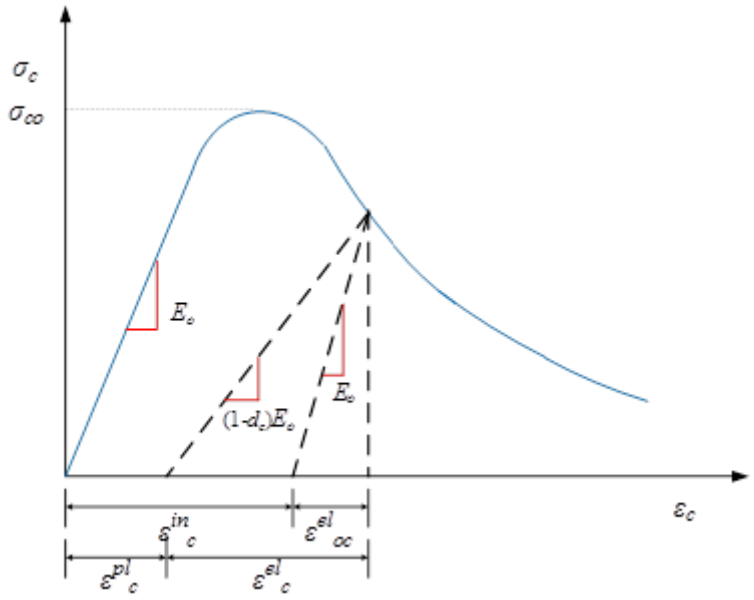

Figure 4 Compression Based Stress - Strain Curve of HFRC

$$d_c = \frac{1}{e^{-1/m_c - 1}}\left(e^{-\varepsilon_{c,norm}^{in}/m_c} - 1\right) \quad (10)$$

The factor m_c in Eq (10), for simple concrete is assigned a value of 0.1 (Huang et al. 2015), as it manages the compression crack development speed, $\varepsilon_{c,norm}^{in}$ is the generalized plastic compressive strain of concrete expressed as: $\varepsilon_c^{in}/\varepsilon_{cu}^{in}$. Further, the normalized inelastic strain of concrete is represented by the compressive strain ε_{cu}^{in} and has an assigned a value of 3.3 x 10^{-2} (Huang, Liew et al. 2015). Therefore, crack propagation speed in HFRC is decreased, in accordance with it. The revised compression governing variable for HFRC is stated by Eq. (11) (Huang, Liew et al. 2015, Chi, Yu et al. 2017).

$$m_c^{hf} = m_c(1 + a_{m1}\lambda_{PVA} + b_{m1}\lambda_{PPF}) \quad (11)$$

Factors a_{m1} and b_{m1} based on characteristic features of fibers have been assigned the values, 4.52 x 10^{-1} and 5.4 x 10^{-2}, respectively (Chi, Yu et al. 2017). The peak compressive stress (σ_{co}^{hf}) and the corresponding compressive strain (ε_{co}^{hf}) of concrete blend can be expressed by the subsequent expressions (Chi, Yu et al. 2017).

$$\sigma_{co}^{hf} = \sigma_{co}(1 + 0.206\lambda_{PVA} + 0.388\lambda_{PPF}) \quad (12)$$

$$\varepsilon_{co}^{hf} = \varepsilon_{co}(1 + 0.705\lambda_{PVA} + 0.364\lambda_{PPF}) \quad (13)$$

3.5.3 Tensile Behavior of HFRC

Strain hardening region of stress-strain curve is depicted by pre-peak region while strain softening region shown by post-peak portion of curve thru plastic (Chi et al. 2014). Figure 5 demonstrates concrete response under tension. (σ_t) known as tensile stress of concrete can be found using Eq. (14) as shown below:

$$\sigma_t = (1 - d_t)E_o\left(\varepsilon_t - \varepsilon_t^{pl}\right) \quad (14)$$

In this relation ε_t and ε_t^{pl} is total strain and plastic strain under tensional load plastic region of concrete. The variable d_t proposed by Wang and Chen (Y 2006) is expressed by Eq. (15) given below.

$$d_t = \frac{1}{e^{-1/m_t - 1}} \left(e^{-\varepsilon_{t,norm}^{ck}/m_t} - 1 \right) \tag{15}$$

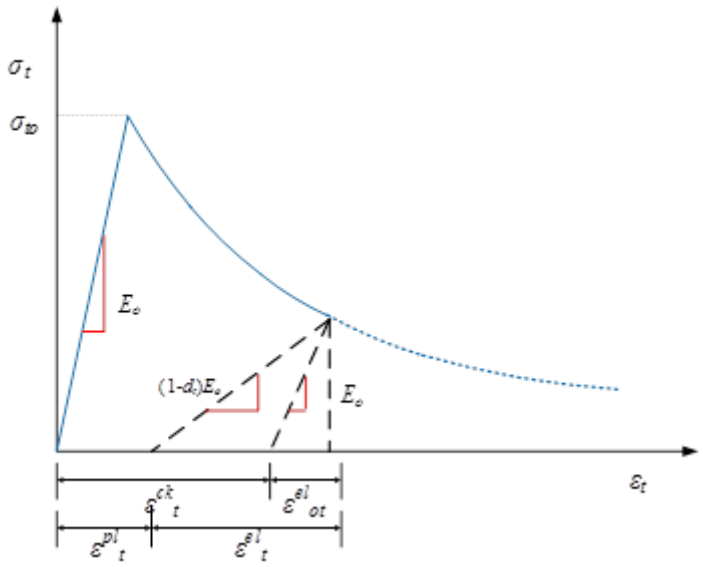

Figure 5 Tensile Stress-Strain Curve of Concrete

In this equation variable m_t manages the tension collapse development speed and for plain concrete 0.05 is its assigned value (Huang, Liew et al. 2015) the factor $\varepsilon_{t,norm}^{ck}$ denotes normal inelastic tensile strain of concrete which can be expressed as: $\varepsilon_t^{ck}/\varepsilon_{tu}^{ck}$. A value of $0.1\varepsilon_{cu}^{in} = 0.0033$ is assigned to inelastic strain developed in concrete represented as tensile strain ε_{tu}^{ck} (Huang, Liew et al. 2015). Crack propagation speed is decreased accordingly in HFRC. For HFRC, the revised tension monitoring expression denoted by (m_t^{hf}) is stated in Eq. (16) (Chi, Yu et al. 2017).

$$m_t^{hf} = m_t(1 + a_{m2}\lambda_{PVA} + b_{m2}\lambda_{PPF}) \tag{16}$$

Factors a_{m2} and b_{m2} with constant value of 0.628 and 0.156 respectively, are based on characteristic properties of PVA and PPF (Huang, Liew et al. 2015). Equation (17) and

(18) presented by (Chi, Yu et al. 2017) are expression to find peak tensile stress (σ_{to}^{hf}) and corresponding tensile strain (ε_{to}^{hf}) of HFRC.

$$\sigma_{to}^{hf} = \sigma_{to}(1 + 0.379\lambda_{PVA} + 0.020\lambda_{PPF}) \quad (17)$$

$$\varepsilon_{to}^{hf} = \varepsilon_{to}(1 + 0.498\lambda_{PVA} + 0.697\lambda_{PPF}) \quad (18)$$

The plastic stress and strain of concrete blend can be found using equations (17) & (18) to give as input data in ABAQUS.

3.6 Assembling & Calibration of GFRP Bars

In modeling software, 3-D truss element type was assigned to the GFRP bar. Characteristic features of reinforcing bars as mentioned in Table 3 like moduli of elasticity, yielding strength and cross-sectional details were given as input. Value of 0.25 was assigned as poison's ratio for GFRP bars (Elchalakani, Karrech et al. 2018). According to (Elchalakani, Karrech et al. 2018, Raza 2019) stress-strain curve is assumed to be linear elastic till failure for GFRP reinforcement. (Zhou et al. 2008) recommended to consider axial compressive strength of GFRP reinforcement as 55% of tensile strength.

3.7 Finite Element Model Validation

Test outcomes of the control specimen (G6-H75) were utilized to assemble and calibrate finite element model (FEM). For various end constraints the projected model was attuned, such as viscosity parameter (μ) of HFRC, mesh size and the element types to achieve close results of the finite element analysis to the experimental results. Predicted result were comparatively close to actual outcomes at lower value of viscosity (μ) (Barth et al. 2006). As depicted in Figure 6(a) the load-deflection graph was found to be influenced by parameter(μ). For viscosity $\mu = 0.0048$, FEA based results were found close to the test results. Value of viscosity parameter should be small enough to

predict better response of the concrete as this is considerably affected by the time increment scale (Raza 2019).

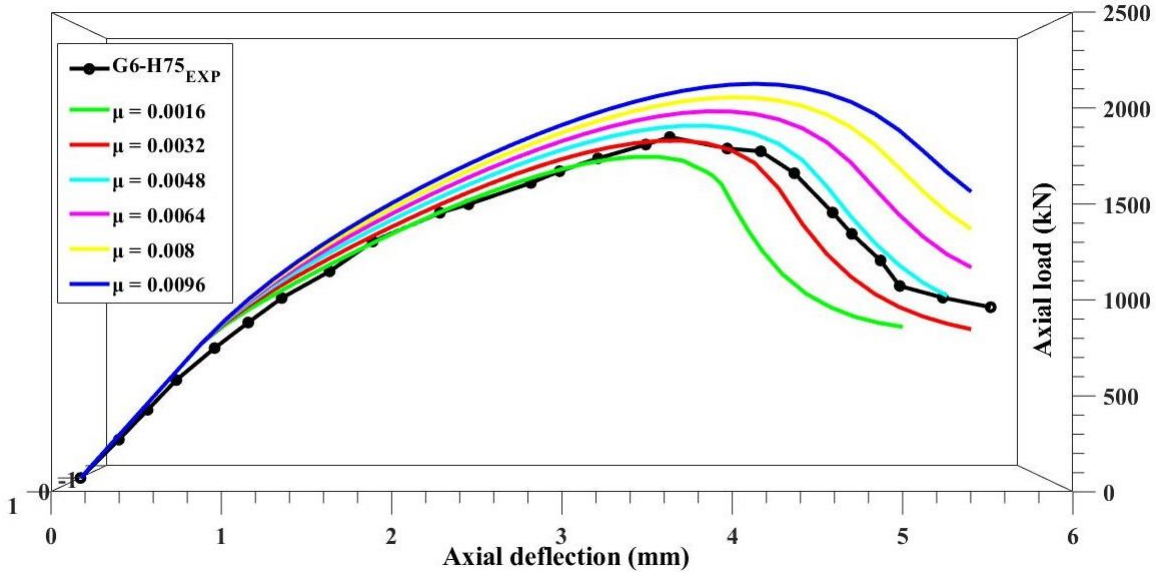

(a)

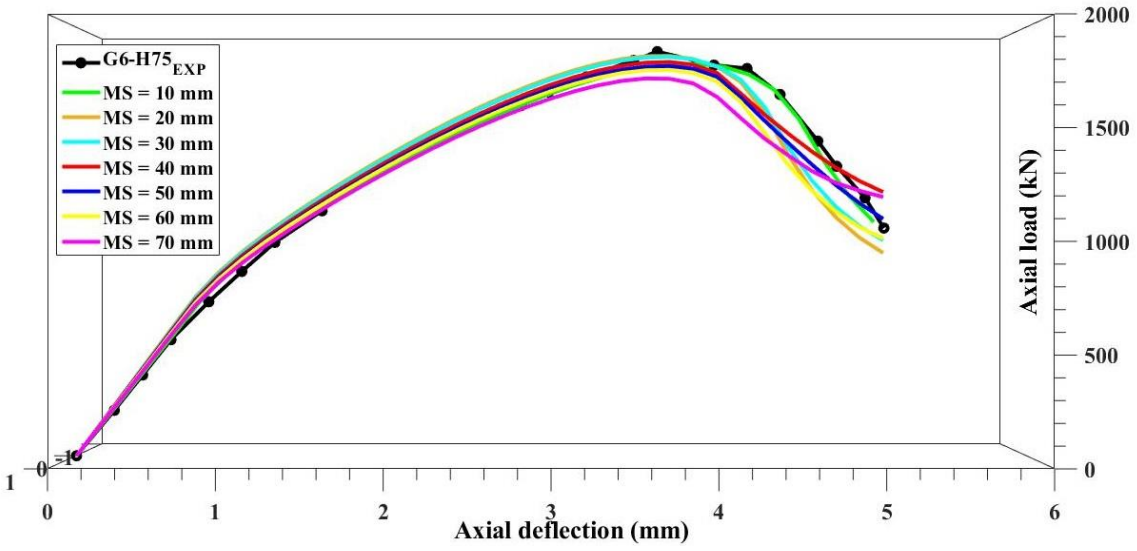

(b)

Figure 6 Influencing Parameter (a) viscosity μ and (b) Effect of Mesh Size on Compressive Behavior

In order to achieve most ideal finite element simulated results, size of mesh was varied to minimize the distortion in the load deflection curve of concrete and reinforcing bars in an appropriate short period of time of FEA. For attaining required results, concrete

model should have a distinctive length. It is clearly visible from the results of load-deflection curve and strain localized forms that these are also dependent on mesh size (Majewski 2008, Jin et al. 2019, Jin et al. 2020). Load-deflection curve is varied on changing size of mesh, clearly visible in Figure 6 (b). Under this study, mesh size was altered from 70 mm to 10 mm with 10 mm constant decrement. For mesh size of 10 mm FEM predicted outcomes were found to be in close agreement to experimental results.

In order to compare and achieve best matching of load deflection curve with respect to the control specimen, concrete and reinforcing bars in FEM model were assigned different element types such as concrete was taken as triangular pyramid (C3D4H & C3D10H), hexahedral (C3D20R & C3D8R), and (C3D6H & C3D15H) triangular types of elements but for element C3D8R most perfect matching of results was attained as supported by studies (Chi, Yu et al. 2017, Raza 2019). Next, GFRP bars was ascribed two types of element T3D3H and T3D2H. Element type T3D2H gave close results to that of experimental results for the reinforcing bars. The effect of changing element types is projected in Figure 7.

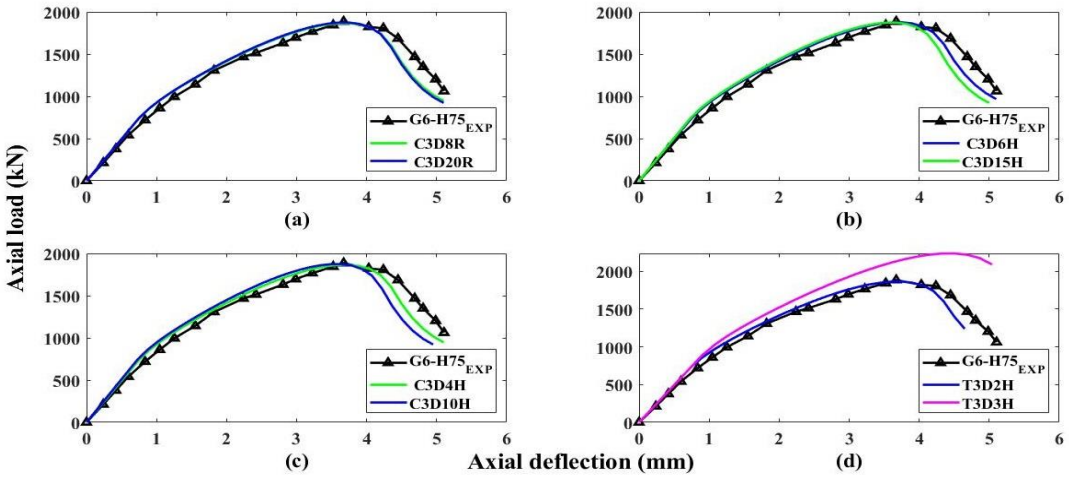

Figure 7 Comparison (a) Hexahedral Element (b) Triangular Element (c) Tetrahedral Element (d) Wire/Truss Element on Compressive Response of the (G6-H75)

3.8 LOAD-CARRYING CAPACITY

3.8.1 Lateral Confinement

Confinement effect of GFRP stirrups increased the bearing strength and ductility of columns(Afifi et al. 2015). In compression members, the contribution of transverse confinement at lower strain is meager, which however, becomes more when the specimen attains ultimate strength, where an increase in lateral strain due to transverse pressure amplified this effect. In the past studies, without bringing into consideration the confinement effect of GFRP ties, the GRFC columns' axial strength was procured. The lateral confining pressure due to GFRP stirrups known as f_l is expressed by Eq. (19) put forward by (Mander et al. 1988).

$$f_l = \frac{A_{ft} f_{fv}}{s d_c} \tag{19}$$

In this equation (19), the cross-sectional area of GFRP stirrups is denoted by A_{ft} , d_c represents the diameter of inner core of column, s is the perpendicular distance among the midpoints of adjacent ties. At unconfined compressive strength of concrete (f'_{co}) GFRP bars are subjected to a pressure f_{fv} which could be found by using equation (20) (Shi et al. 2014).

$$f_{fv} = 0.30 \left(\frac{E_f k_e \rho_t}{f'_{co}}\right)^{1.57} + 26.60 \tag{20}$$

In the equation (20), the volumetric ratio of GFRP lateral reinforcement is represented by factor ρ_t while the young's modulus of GFRP lateral ties is denoted by factor E_f while the degree of effective confinement is represented by the variable k_e. While considering parabolic effect owing to confinement nature of stirrups a model was suggested by (Mander, Priestley et al. 1988) for this variable as shown in Figure 8.

A 2nd degree parabolic profile is attained due to this curving effect (Mander, Priestley et al. 1988, Afifi, Mohamed et al. 2015).

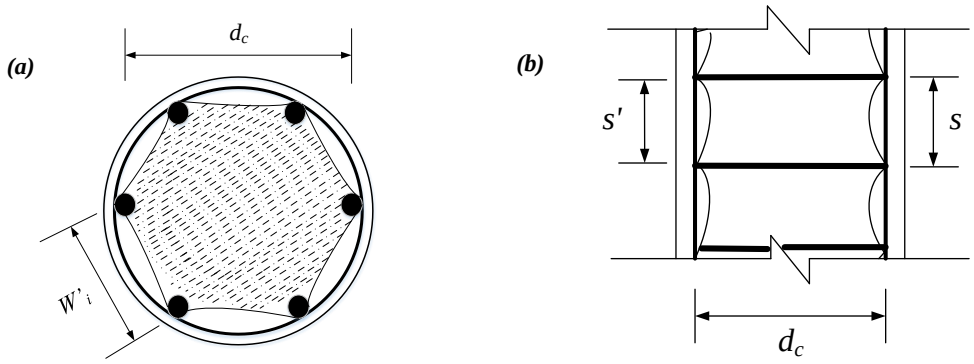

Figure 8 Confinement of GFRP (a) Cross-section of Column (b) Sideway View

$$k_e = \frac{\left(1-\sum_{i=1}^{n}\frac{(w_i')^2}{6d_c^2}\right)\left(1-\frac{s'}{2d_c}\right)^2}{1-\rho_l} \tag{21}$$

In this expression for k_e, the factor w_i' denotes perpendicular distance amid the longitudinal GFRP bars, pitch of GFRP ties is depicted by factor s' and the reinforcement ratio of GFRP bars is represented by the variable ρ_l. (Mander, Priestley et al. 1988) predicted the effective lateral confining pressure (f_{le}), as presented in equation (22).

$$f_{le} = k_e f_l \tag{22}$$

The variables f_l and k_e can be procured by using equation (20) and equation (22), respectively. The axial stress of FRP tied concrete columns to be found using equation (23) put forward by (Ahmad and Raza 2020) to find compressive strength of confined concrete (f'_{cc}). The strain model put forward by (Raza et al. 2020b), equation (24), for fiber reinforced polymer tied columns was utilized to calculate the axial strain of confined concrete under compression (ε'_{cc}).

$$\frac{f'_{cc}}{f'_{co}} = 1.0 + 3.1\left(\frac{f_{le}}{f'_{co}}\right)^{0.83} \tag{23}$$

$$\frac{\varepsilon'_{cc}}{\varepsilon'_{co}} = 1.85 + 7.46{\rho_k}^{0.71}{\rho_\varepsilon}^{1.17} \quad (24)$$

The equations (25) and (26) represent the variables ρ_k known as confinement stiffness ratio and variable ρ_ε known as strain ratio, used in equation (24), respectively (Teng et al. 2009).

$$\rho_\varepsilon = \frac{\varepsilon_{h,rup}}{\varepsilon_{co}} \quad (25)$$

$$\rho_k = \frac{2E_f t}{\left(\frac{f'_{co}}{\varepsilon_{co}}\right)D} \quad (26)$$

Factor f'_{co} in equation (26) is unconfined concrete's peak strength, variable ε'_{co} denotes unconfined concrete's compressive strain with respect to ultimate loading strength, variable ε'_{cc} is the maximum strain for laterally GFRP tied concrete columns, modulus of elasticity of confinement cover present transversely to cylinders is symbolized by factor E_f, t symbolizes thickness of FRP bars or sheet, f'_{co} symbolizes compressive stress of unconfined concrete and ε_{co} symbolizes compressive strain of unconfined concrete. Failure strain of confining stirrup bars represented by a mathematical equation (27) was proposed by (Lim et al. 2016).

$$\varepsilon_{h,rup} = \frac{\varepsilon_f}{f'^{0.125}_{co}} \quad (27)$$

In this expression, ε_f denotes the ultimate tensile strain in fibres.

3.9 Proposed Equation

Certain number of models presented in the literature (Attard and Setunge 1996, Pantelides et al. 2013, Afifi, Mohamed et al. 2014, Mohamed, Afifi et al. 2014, Tobbi, Farghaly et al. 2014, Hadhood, Mohamed et al. 2017, Khan et al. 2017) are utilized to unearth the load bearing capacity of fiber reinforced polymer concrete columns. Except of the final models put forward by (Pantelides, Gibbons et al. 2013, Khan, Sheikh et al.

2017) for GFRP reinforced ordinary concrete columns, equation presented by a lot of other researchers neglected the effect of GFRP bars' confinement effect. Most of the models have assumed peak axial compressive strain of concrete and GFRP bars alike (Pantelides, Gibbons et al. 2013, Tobbi, Farghaly et al. 2014).

The numerical findings demonstrated under estimation of axial compressive strength of GFRP reinforced columns as we neglect the lateral confining pressure owing to transverse ties. To forecast peak compressive strength of GRFC columns by undertaking confinement effect of transverse ties, this study helped to propose an empirical relation while taking maximum axial stress and strain of GFRP bars and HFRC equal as shown in equation (28).

$$P_n = 0.85f'_{cc}\left(A_g - A_{FRP}\right) + \varepsilon'_{cc}E_{FRP}A_{FRP} \quad (28)$$

The factor A_g in the equation symbolizes specimen's gross cross-sectional area, factor A_{FRP} represents the overall cross-sectional area of longitudinal GFRP bars, and factor E_{FRP} denotes elastic modulus of GFRP bars.

Chapter 4

RESULTS DISCUSSION

4.1 Peak Loads and Relative Deflections

Outline of test results and numerical based predictions achieved by using FEM for GRFC concentrically loaded columns is depicted in Table 4-1. The maximum variation of FEM simulation to test results for peak compressive strength was perceived for G6-S38 with a standard deviation of 4.49%. At peak compressive strength, in case of G6-H250 a standard deviation of 10.22% was detected for vertical deflection. The initial geometric imperfectness which were not dealt in finite element modelling were considered the reason of large differences. For GRFC columns the average variance amid the test results and FEA predictions were 2.61% for peak compressive strength and 4.63% for vertical deflection at peak applied load. The peak compressive strength of samples assembled in FEM displayed lower value in majority of the cases. Thus, the GRFC columns displayed a decent structural performance.

Table 4-1 Experimental & Numerical Results

Label	Experimental results		FEA results		%age	%age
	Ultimate load (KN)	Axial deflection at ultimate load (mm)	Ultimate load (KN)	Axial deflection at ultimate load (mm)	difference in ultimate load	difference in deflection at ultimate load
G6-H75	1885.04	3.67	1864.92	3.75	1.07	2.18
G6-H150	1638.16	3.37	1588.60	3.59	3.03	6.53
G6-H250	1760.65	3.13	1814.74	3.45	3.07	10.22
G6-S38	2231.75	4.72	2131.48	4.63	4.49	1.91
G6-S75	2002.95	4.77	1974.80	4.88	1.41	2.31

Figure 9 demonstrates the load-deflection curves, both the experimentally obtained and the numerical one, of concentrically loaded GRFC columns. The response predicted by FEM model of concentrically loaded GRFC columns showed minor variances both in pre and post peak region of curve. The FEM simulation results related to load-deflection behavior of some specimens, i.e. G6-S38 and G6-H75, disclosed that their elastic region had additional stiffness. It can be noticed that in the post-peak region of the curve, the FEM predictions vary slightly from the test results. This specimens' behavior perhaps can be ascribed to complex failure response of concrete after spalling and relation between GFRP bars and HFRC requires additional perfection.

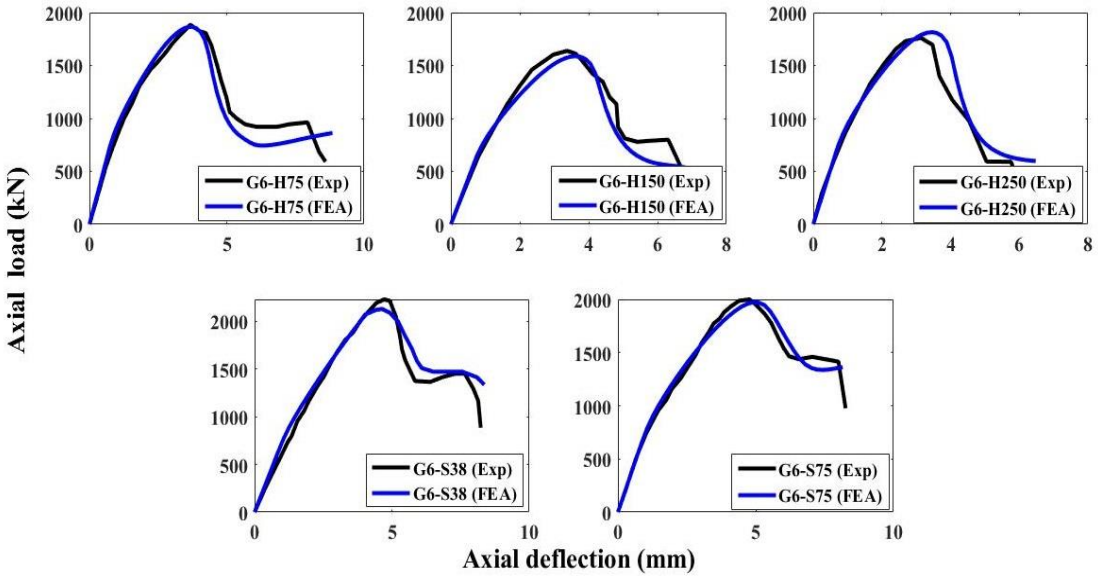

Figure 9 Comparison of Stress-Strain Curves of GRFC Columns (Exp. And FEM)

4.2 Collapse Patterns

The collapse appeared to initiate in the upper half region of all the specimens. During the application of axial load, until the 75% of the peak strength, the casted columns remained elastic, and the confinement rupture was not initiated. With further increase in the applied load, cracking of HFRC initiated with delicate feeble sound, and longitudinal thin crack began at the upper region of the tested columns. As the application of load was further intensified, the width of minor cracks amplified until

the maximum value was reached. At the maximum applied loading, vertical deflection of the specimens amplified at an increased speed triggering extended ruptures along the columns' height. At this stage, the spalling of concrete initiated, and leading to failure of the lateral ties. Transverse ties attained their peak capacity raising a fracture sound in GRFC specimens with a reduction in loading capacity of the columns up till 60% of the peak capacity.

Figure 10 shows the failure propagation patterns of casted samples and assembled FEM. While performing FEM, at the maximum value of positive plastic strains, there were cracks in the concrete observed. Rupture pattern is efficiently traced as the splitting track is mostly normal to usual strains (Genikomsou and Polak 2015, Raza 2019, Ahmad and Raza 2020, Raza, Shah et al. 2020b). The failure pattern of FEM based assembled columns seemed to be adequate. The spalling of concrete cover was initiated as the column attains the peak load. In addition to this, yielding was initiated by longitudinal bars, along with collapse propagation. It is clear from the results of the column samples collected, that the key or in other words the crucial failure portion is the upper region. The evidence also shows that the FEM anticipated the failure of the columns similar to the test results.

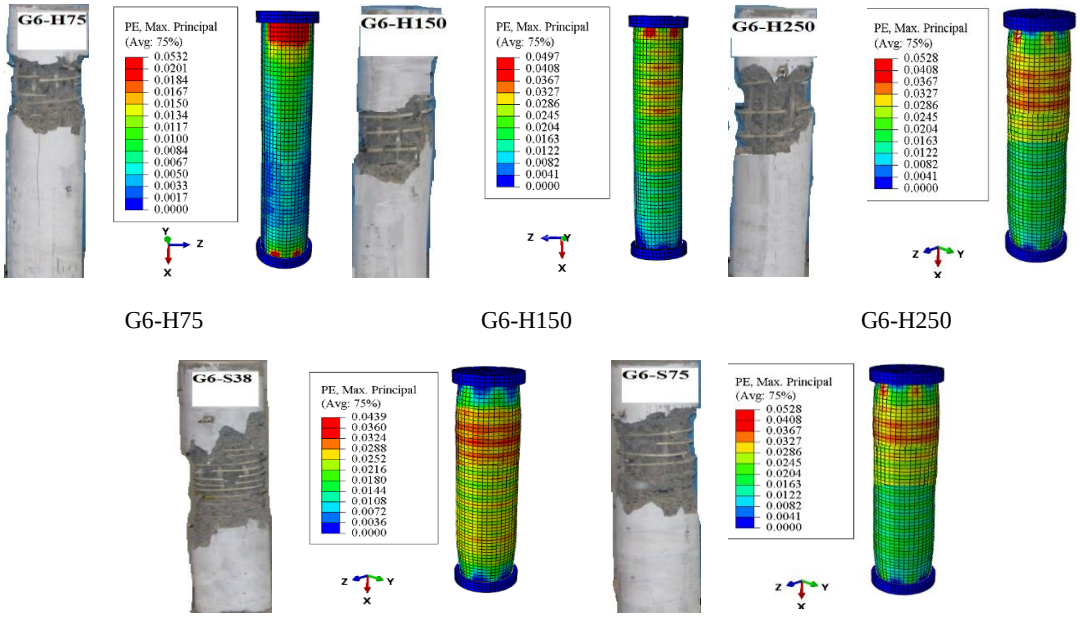

Figure 10 Failure Rundown of GRFC Columns

4.3 Columns' Ductility Index

With the employment of equation (29) (Hadi and Youssef 2016a, Elchalakani and Ma 2017, Elchalakani et al. 2019) the ductility indices of the columns were calculated in this study.

$$I = \frac{A_{\Delta 85}}{A_{\Delta 75}} \tag{29}$$

The area under the axial load-deflection curve up to Δ_{75}, is represented by the variable $A_{\Delta 75}$ in this equation, where Δ_{75} is the value of the amount of axial deflection of the sample in the straight-line portion of the load-deflection curve, under the effect of 75% of the maximum load. Variable $A_{\Delta 85}$ denotes area below stress-strain curve till Δ_{85}, where Δ_{85} designates the axial deflection of the specimen in the downgrading portion of load-declination curve corresponding to 0.85 times the maximum load.

Figure 10 illustrates experimentally tested columns' ductility index. The chart clearly illustrates decrease in ductility with rise in pitch of transverse reinforcement. It is clear

from the bar chart that, with a reduction in the stirrups spacing the ductility index rises. For columns with transverse ties, with stirrup pitches of 250mm, 150mm and 75mm, ductility indices were 2.34, 2.58 and 2.97 respectively. The efficient confinement of the concrete core which proves to be effective in absorbing the extra energy is attributed to be the reason of increase in columns' ductility with decrease in its pitch (Elchalakani, Dong et al. 2019).

For laterally confined GRFC columns with spirals, the ductility index with pitch of 38 mm and 75 mm came out to be 3.19 and 2.94 respectively. This portrays that an increase in ductility is showed by the specimens that are confined with closely spaced GFRP spirals, in contrast to the column specimens with a higher pitch of spirals.

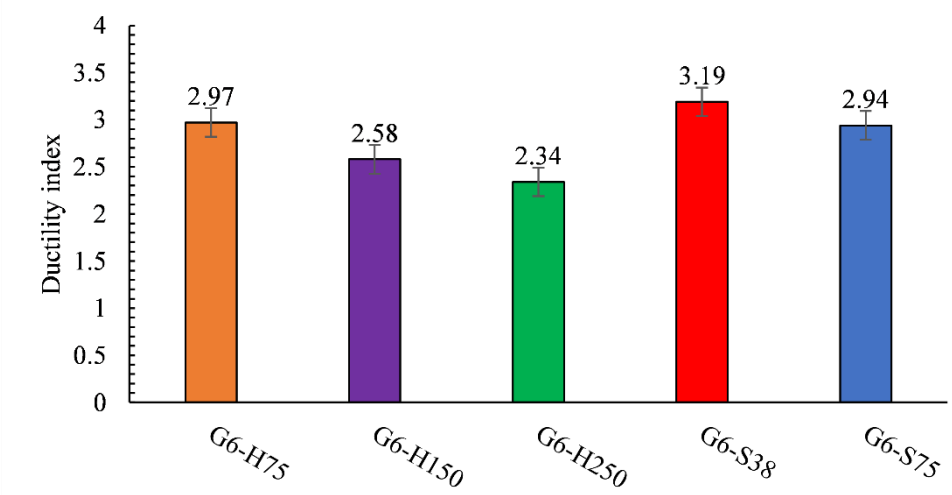

Figure 11 Ductility Indices of GRFC Specimens

4.4 Effect of The Type of Lateral Reinforcement

In contrast to GFRP ties, GFRP spirals offered better performance. Mean compressive axial strength of spirally confined GFRP columns found out to be 116.82% as compared hoop ties columns. Likewise, limit of vertical deflection presented by spirally confined columns was higher at the ultimate load carried by the specimens. The mean of axial divergence of spirally reinforced column with respect to ultimate load was 128.63% in

comparison to columns with hoop ties. Higher axial compressive strength is attained by columns due to enhanced continuous lateral confinement of the concrete core provided by both lateral and longitudinal GFRP reinforcement. The load carrying strength of G6-S75 came out to be 105.88% to that of a similar GFRP tied column (G6-H75). Further, it may also be a reason that, with decrease in the vertical spacing of spirals in columns (G6-S38 and G6-S75) there is a surge in axial strength of the specimens. Thus, for the HFRC columns with longitudinal GFRP bars it is more effective to provide GFRP spirals.

4.5 Pitch Variation Effect

(Elchalakani and Ma 2017, Elchalakani, Dong et al. 2019)reported in studies, that GRFC columns' loading capacity is enhanced with reduction in pitch of transverse ties. The axial strength of GRFC concentrically loaded columns increased by 13.09% on reducing ties' spacing from 150 mm (0.71% volume of stirrups) to 75 mm (1.42% volume of stirrups), under concentric loading. This improved axial strength of columns at reduced pitch of stirrups is associated to effective transverse confinement of the concrete confined within ties known as concrete core and efficiently constrained longitudinal GFRP reinforcing bars (Elchalakani, Dong et al. 2019). Further, it came out that the GRFC concentrically loaded columns' axial strength reduced by 7.47% when stirrups spacing of 250 mm was dropped down to 150 mm (which is a decrease in volumetric amount of 0.21% for stirrups). Thus, it was clearly and efficiently demonstrated that a better loading strength was exhibited by the GFRP-RC columns when there was a reduction in pitch of stirrups.

4.6 Validation of Proposed Equation

A comparison is drawn regarding the ultimate capacity of specimens as obtained by experimental testing, FEM and empirical analysis in Figure 12. A comparative study

disclosed that the recently proposed empirical model predicted the ultimate strength of GRFC columns with greater accuracy. Predictions made by the empirical models put forward by (Attard and Setunge 1996, Pantelides, Gibbons et al. 2013, Afifi, Mohamed et al. 2014, Mohamed, Afifi et al. 2014, Tobbi, Farghaly et al. 2014, Hadhood, Mohamed et al. 2017, Khan, Sheikh et al. 2017) contrasted from test results by mean per centum of 11.59%, 31.34%, 8.88%, 11.15%, 11.51%, 10.77% and 9.81%, respectively. Concentrically loaded GRFC columns showed a standard variance of 5.69%, by the recently proposed empirical relation for predicting the compressive load carrying capacity of columns. The projections put forward by the recently proposed empirical relation and FEM vary by mean percentage of 10.63%. Thus, by considering the conduct of GFRP transverse confinement, load carrying strength of columns made up of GRFC can be efficiently predicted by the proposed empirical relation.

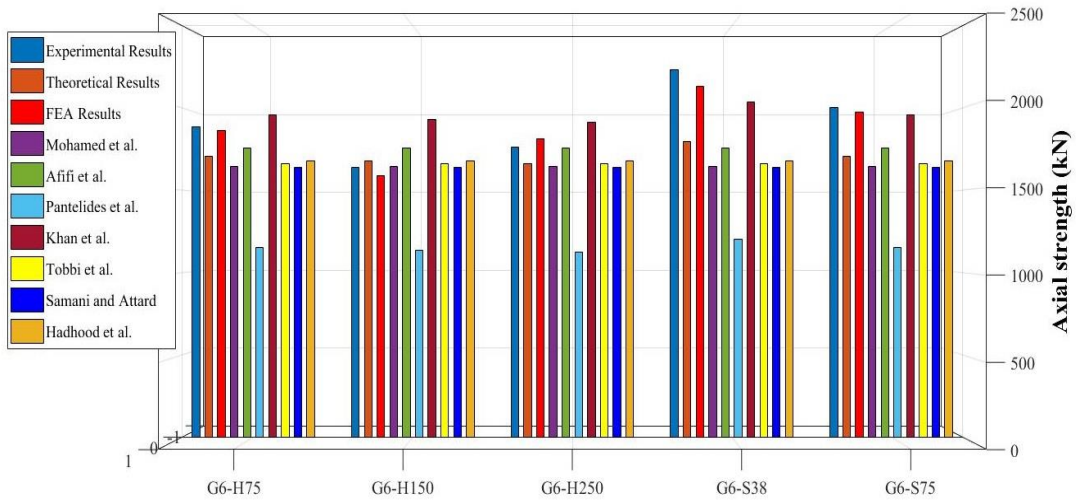

Figure 12 Ultimate Axial Capacity of Column Specimens Achieved from Experimental, Empirical & FEM Results

Chapter 5

CONCLUSIONS

Objective of this research was to explore the structural behavior of GRFC concentrically loaded columns by experimental testing, FEA as well as by empirical assessment. The conclusions drawn from this study are:

1. The process as well as the modes of failure observed in all GRFC columns was same. The columns mostly showed failure in their upper half due to the rupture of longitudinal reinforcement.

2. Concrete columns made with GFRP reinforced recycled aggregate fiber-incorporated concrete (GRFC) did great as regards as the axial load-carrying capacity, modes of failure as well as ductility. This is why, they can be utilized in GFRP-RC columns for design purposes.

3. Close spacing of the stirrups, remarkably increased the columns' ductility index as it resulted in concrete core's effective confinement which in turn led to absorption of additional energy and also because the longitudinal reinforcement was firmly restrained. Ductility indices presented by spirally confined concrete columns was higher in comparison to tied columns.

4. Reducing the hoops'/stirrups' spacing, improved the GRFC columns' axial strength. The GRFC columns showed an increase of 13.09% in their axial strength by reducing stirrup spacing from 150 mm to 75 mm, whereas on reducing pitch from 250 mm to 150 mm, the axial strength decreases by 7.47%. Lastly, in case of spirally reinforced column a boost of 10.25% in compressive strength was marked as pitch was downgraded to 38 mm from 75 mm.

5. On assigning modified CDP model (plastic fiber-based) to HFRC the apparent versatile behavior was very accurately predicted by the suggested FEM. A mean proportional error suggested by FEM, for the axial loading capacity and the corresponding axial strain of the specimens under study, was showed to be 2.61% and 4.63%, respectively. In order to simulate crack propagation and failure modes of column specimens under study accurately, ABAQUS was employed.

The recently suggested theoretical model regarding the GFRC columns' axial strength did remarkably well by considering the axial effect produced by GFRP bars as well as the lateral confining input of the GFRP ties. The discrepancies from experimental observations as well as finite element assessment regarding samples' loading strength were of a mean percentage of almost 5.69% and 10.63% respectively. Therefore, in order to get a better structural response, recycled coarse aggregates are a good choice to be utilized alongside hybrid fibers while making GFRP reinforced columns.

REFERENCES

Abdelrahman, K. and R. El-Hacha (2014). "Cost and Ductility Effectiveness of Concrete Columns Strengthened with CFRP and SFRP Sheets." **6**(5): 1381-1402.

ACI-318 (1995). Building Code Requirements for Structural Concrete. Farmington Hills: MI:.

Afifi, M. Z., et al. (2014). "Axial Capacity of Circular Concrete Columns Reinforced with GFRP Bars and Spirals." **18**(1): 04013017.

Afifi, M. Z., et al. (2015). "Theoretical stress–strain model for circular concrete columns confined by GFRP spirals and hoops." **102**: 202-213.

Ahmad, A. and A. J. C. S. Raza (2020). "Reliability analysis of strength models for CFRP-confined concrete cylinders." **244**: 112312.

Attard, M. and S. J. M. J. Setunge (1996). "Stress-strain relationship of confined and unconfined concrete." **93**(5): 432-442.

Barth, K. E., et al. (2006). "Efficient nonlinear finite element modeling of slab on steel stringer bridges." **42**(14-15): 1304-1313.

Bayramov, F., et al. (2004). "Optimisation of steel fibre reinforced concretes by means of statistical response surface method." **26**(6): 665-675.

Benmokrane, B., et al. (2006). "Designing and testing of concrete bridge decks reinforced with glass FRP bars." **11**(2): 217-229.

Boscato, G. and S. J. C. S. Ientile (2018). "Experimental and numerical investigation on dynamic properties of thin-walled GFRP buckled columns." **189**: 273-285.

Boumarafi, A., et al. (2015). "Harsh environments effects on the axial behaviour of circular concrete-filled fibre reinforced-polymer (FRP) tubes." **83**: 81-87.

Chi, Y., et al. (2014). "Constitutive modeling of steel-polypropylene hybrid fiber reinforced concrete using a non-associated plasticity and its numerical implementation." **111**: 497-509.

Chi, Y., et al. (2014). "Plasticity model for hybrid fiber-reinforced concrete under true triaxial compression." **140**(2): 393-405.

Chi, Y., et al. (2017). "Finite element modeling of steel-polypropylene hybrid fiber reinforced concrete using modified concrete damaged plasticity." **148**: 23-35.

Chi, Y., Yu, M., Huang, L., Xu, L. (2017). "Finite element modeling of steel-polypropylene hybrid fiber reinforced concrete using modified concrete damaged plasticity." Engineering Structures **148**: 23-35.

Choi, W.-C. and H.-D. J. E. s. Yun (2012). "Compressive behavior of reinforced concrete columns with recycled aggregate under uniaxial loading." **41**: 285-293.

Choo, C. C., et al. (2006). "Strength of rectangular concrete columns reinforced with fiber-reinforced polymer bars." **103**(3): 452.

Darole, J., et al. (2013). "Effect of hybrid fiber on mechanical properties of concrete." **3**(4): 1408-1411.

Elchalakani, M., et al. (2019). "Experimental investigation of rectangular air-cured geopolymer concrete columns reinforced with GFRP bars and stirrups." **23**(3): 04019011.

Elchalakani, M., Dong, M., Karrech, A., Li, G., MS Mohamed A., Yang, B. (2019). "Experimental Investigation of Rectangular Air-Cured Geopolymer Concrete Columns Reinforced with GFRP Bars and Stirrups." Journal of Composites for Construction **23**(3): 04019011.

Elchalakani, M., et al. (2018). Experiments and finite element analysis of GFRP reinforced geopolymer concrete rectangular columns subjected to concentric and eccentric axial loading. Structures, Elsevier.

Elchalakani, M., et al. (2021). "Testing and modelling of geopolymer concrete members with fibreglass reinforcement." **174**(1): 12-27.

Elchalakani, M. and G. J. E. S. Ma (2017). "Tests of glass fibre reinforced polymer rectangular concrete columns subjected to concentric and eccentric axial loading." **151**: 93-104.

Genikomsou, A. S. and M. A. J. E. s. Polak (2015). "Finite element analysis of punching shear of concrete slabs using damaged plasticity model in ABAQUS." **98**: 38-48.

Hadhood, A., et al. (2017). "Axial load–moment interaction diagram of circular concrete columns reinforced with CFRP bars and spirals: Experimental and theoretical investigations." **21**(2): 04016092.

Hadi, M. N., et al. (2016). "Experimental investigations on circular concrete columns reinforced with GFRP bars and helices under different loading conditions." **20**(4): 04016009.

Hadi, M. N. and J. J. J. o. C. f. C. Youssef (2016a). "Experimental investigation of GFRP-reinforced and GFRP-encased square concrete specimens under axial and eccentric load, and four-point bending test." **20**(5): 04016020.

Hales, T. A., et al. (2017). "Analytical buckling model for slender FRP-reinforced concrete columns." **176**: 33-42.

Hany, N. F., et al. (2016). "Finite element modeling of FRP-confined concrete using modified concrete damaged plasticity." **125**: 1-14.

Hastemoglu, H. J. J. C. E. E. (2015). "Effect of recycled aggregate on the compressive behavior of short concrete columns." **5**(6): 1000194.

Huang, Z., et al. (2015). "Nonlinear finite element modelling and parametric study of curved steel–concrete–steel double skin composite panels infilled with ultra-lightweight cement composite." **95**: 922-938.

Jiang, D., et al. (2018). "Analysis and design of floating prestressed concrete structures in shallow waters." **59**: 301-320.

Jin, L., et al. (2020). "Size effect on nominal strength of circular stirrup-confined RC columns under axial compression: Mesoscale study." **146**(3): 04019213.

Jin, L., et al. (2019). "Size effect in shear failure of RC beams with stirrups: Simulation and formulation." **199**: 109573.

Khan, Q. S., et al. (2017). "Axial-flexural interactions of GFRP-CFFT columns with and without reinforcing GFRP bars." **21**(3): 04016109.

Kim, S.-W., et al. (2013). "Size effect in shear failure of reinforced concrete beams with recycled aggregate." **12**(2): 323-330.

Li, W., et al. (2018). "Impact performances of steel tube-confined recycled aggregate concrete (STCRAC) after exposure to elevated temperatures." **86**: 87-97.

Li, W., et al. (2017). "Experimental and numerical studies on impact behaviors of recycled aggregate concrete-filled steel tube after exposure to elevated temperature." **136**: 103-118.

Li, W., et al. (2015). "Structural behaviour of composite members with recycled aggregate concrete—an overview." **18**(6): 919-938.

Lim, J. C., et al. (2016). "Evaluation of ultimate conditions of FRP-confined concrete columns using genetic programming." **162**: 28-37.

Liu, J., et al. (2020). "Economic and Environmental Assessment of Carbon Emissions from Demolition Waste Based on LCA and LCC." **12**(16): 6683.

Lu, K. (2011). "Modelling of multicomponent diffusion and swelling in protein gels."

Ma, H., et al. (2013). "Seismic performance of steel-reinforced recycled concrete columns under low cyclic loads." **48**: 229-237.

Majewski, T. J. F. a. o. f. b. o. r. c. c. u. e. c., Eng. Struct (2008). "Bobinski and J. Tejchman." **30**(2): 300-317.

Mander, J. B., et al. (1988). "Theoretical stress-strain model for confined concrete." **114**(8): 1804-1826.

Maranan, G., et al. (2016). "Behavior of concentrically loaded geopolymer-concrete circular columns reinforced longitudinally and transversely with GFRP bars." **117**: 422-436.

Mohamed, H. M., et al. (2014). "Performance evaluation of concrete columns reinforced longitudinally with FRP bars and confined with FRP hoops and spirals under axial load." **19**(7): 04014020.

Pang, Y., et al. (2019). "Seismic performance assessment of different fibers reinforced concrete columns using incremental dynamic analysis." **203**: 241-257.

Pantelides, C. P., et al. (2013). "Axial load behavior of concrete columns confined with GFRP spirals." **17**(3): 305-313.

Paultre, P., et al. (2010). "Behavior of steel fiber-reinforced high-strength concrete columns under uniaxial compression." **136**(10): 1225-1235.

Raza, A., et al. (2021). "Concentrically loaded recycled aggregate geopolymer concrete columns reinforced with GFRP bars and spirals." **268**: 113968.

Raza, A. and U. J. C. S. Rafique (2021). "Efficiency of GFRP bars and hoops in recycled aggregate concrete columns: Experimental and numerical study." **255**: 112986.

Raza, A., et al. (2020b). "Sustainable FRP-confined symmetric concrete structures: an application experimental and numerical validation process for reference data." **10**(1): 333.

Raza, A., et al. (2020a). Finite element modelling and theoretical predictions of FRP-reinforced concrete columns confined with various FRP-tubes. Structures, Elsevier.

Raza, A. J. A. i. C. E. (2019). "Q. u. Z. Khan, and A. Ahmad,"Numerical investigation of load-carrying capacity of GFRP-reinforced rectangular concrete members using CDP model in ABAQUS,"." **2019**.

Raza, A. J. S. A. S. (2020). "Experimental and numerical behavior of hybrid-fiber-reinforced concrete compression members under concentric loading." **2**(4): 1-19.

Shi, Q., et al. (2014). "A practical stress-strain model for high-strength stirrups confined concrete." **17**(2): 216-222.

Shi, Y., et al. (2012). "Modelling damage evolution in composite laminates subjected to low velocity impact." **94**(9): 2902-2913.

Silva, N., et al. (2011). "First-order, buckling and post-buckling behaviour of GFRP pultruded beams. Part 2: Numerical simulation." **89**(21-22): 2065-2078.

Teng, J., et al. (2009). "Refinement of a design-oriented stress–strain model for FRP-confined concrete." **13**(4): 269-278.

Tobbi, H., et al. (2014). "Behavior of Concentrically Loaded Fiber-Reinforced Polymer Reinforced Concrete Columns with Varying Reinforcement Types and Ratios." **111**(2).

Turvey, G., et al. (2006). "A computational and experimental analysis of the buckling, postbuckling and initial failure of pultruded GRP columns." **84**(22-23): 1527-1537.

Wang, B., et al. (2021). "A Comprehensive Review on Recycled Aggregate and Recycled Aggregate Concrete." **171**: 105565.

Wang, Y., et al. (2015). "Testing and analysis of axially loaded normal-strength recycled aggregate concrete filled steel tubular stub columns." **86**: 192-212.

Xu, J.-J., et al. (2017). "Recycled aggregate concrete in FRP-confined columns: a review of experimental results." **174**: 277-291.

Y, W. J. (2006). "ABAQUS Application in Civil Engineering." Hangzhou: Zhejiang University Press.

Zhang, C., et al. (2018). "Flexural performance of reinforced self-consolidating concrete beams containing hybrid fibers." **174**: 11-23.

Zhou, J.-k., et al. (2008). "Experimental study on compressive mechanical properties of GFRP rebars." **4**: 542-545.